Polish Society of Composite Materials
Polskie Towarzystwo Materiałów Kompozytowych

19: 3 (2019) 119-125

COMPOSITES THEORY AND PRACTICE
ISSN: 2084-6096
ISSN (online): 2299-128X

Dominik Banat

Department of Strength of Materials, Lodz University of Technology, ul. Stefanowskiego 1/15, 90-924 Lodz, Poland
Corresponding author. E-mail: dominikbanat@gmail.com

Received (Otrzymano) 4.08.2019

FLEXURAL PERFORMANCE OF FIBRE REINFORCED COMPOSITE BEAMS - NUMERICAL ANALYSIS

This paper deals with multi-layered FRP composite beams subjected to the three-point bending test. The study is focused on the flexural performance of rectangular composite beams made of glass or carbon fibre-reinforced laminates (GFRP and CFRP). Depending on the fibre orientation, various laminate systems were analysed with the main focus on $[0_8]_T$ and $[90_8]_T$ layups. Tests on three beams with different length-to-thickness ratios included a three-point short beam shear test (SBS), assuming a relatively short beam is in relation to its thickness, which maximized the induced shear stresses. Additionally, two variants of boundary conditions were discussed with layers oriented parallel and perpendicular to the loading plane. Geometrically nonlinear analysis aimed to verify the load-midspan deflection curves for various fibre-reinforced composite beams was performed. The presented initial results concern comparative numerical analysis performed by the finite element method (FEM), which is found to be crucial before further experimental research.

Keywords: fibre reinforced polymer (FRP), composite material, glass fibre, carbon fibre, flexural test, numerical simulation

WYTRZYMAŁOŚĆ NA ZGINANIE BELEK WYKONANYCH Z KOMPOZYTÓW WŁÓKNISTYCH - ANALIZA NUMERYCZNA

Artykuł dotyczy wielowarstwowych belek kompozytowych typu FRP poddanych trzypunktowej próbie zginania. Badania koncentrują się na wytrzymałości na zginanie prostokątnych belek kompozytowych wykonanych z kompozytów włóknistych wzmacnianych włóknem szklanym lub węglowym (GFRP i CFRP). W zależności od kierunku ułożenia włókien analizie poddano różne konfiguracje laminatów ze szczególnym uwzględnieniem układów $[0_8]_T$ i $[90_8]_T$. Analizę numeryczną wykonano dla trzech belek o różnych stosunkach długości do grubości, w tym również trzypunktowy test zginania krótkiej belki (SBS) w celu zmaksymalizowania naprężeń ścinających. Dodatkowo przedstawiono dwa warianty warunków brzegowych z warstwami ułożonymi równolegle lub prostopadle do płaszczyzny obciążenia. Przeprowadzono geometryczną analizę nieliniową w celu zweryfikowania krzywych obciążenie-ugięcie dla różnych wariantów belek wykonanych z kompozytów włóknistych. Przedstawione wstępne wyniki dotyczą porównawczej analizy numerycznej, wykonanej z zastosowaniem metody elementów skończonych (MES), która ma kluczowe znaczenie przed dalszymi badaniami eksperymentalnymi.

Słowa kluczowe: kompozyt włóknisty, materiały kompozytowe, włókno szklane, włókno węglowe, test zginania, symulacja numeryczna

INTRODUCTION

Glass or carbon fibre-reinforced composites (GFRP and CFRP) are recognized as one of the most commonly applied structural materials that have been increasingly used in recent years. Significant developments are observed in the aerospace, automotive, sport equipment, civil and transport industries [1]. Therein, multifunctional composite structures tend to replace traditional materials such as steel or aluminium. This is caused by the growing demand for lightweight and high strength materials that need to meet the high requirements of modern industries [2, 3]. Fibre-reinforced polymers (FRP) are found to guarantee improved strength and stiffness, especially when compared to other structural materials on a unit weight basis. Furthermore, different ply combinations within FRP composites provide high bearing strength and improved impact resistance [4]. The fibre alignment and fibre volume ratio also affect the overall performance of the composite [5]. This provides FRPs that could be stiffer in one particular direction, which gives several advantages for its industrial applications [6].

In literature, one can find various papers concerning the theoretical and experimental studies of different thin-walled composite structures subjected to compressive loading [7, 8]. However, another fundamental property that determines FRP performance is high flexural strength, which leads to the need to perform strength analysis optimization [9, 10]. Therefore, an

attempt has been taken to analyse the flexural strength of various composite materials for which the short beam shear (SBS) method is most commonly applied in the three-point bending test [11-13]. Herein, depending on the beam's span-to-thickness ratio, the beam performance is governed by induced normal and shear stresses or by their combined effect [14, 15]. To analyse longer beams (l/h = 32 or higher), the three-point and four-point bending test are commonly applied to investigate beam flexural performance [16]. Nevertheless, the aforementioned SBS test was primarily focused on only three-point tests and no advantage is found in using four-point loading for a short beam investigation [17].

The aim of this study is to investigate the flexural performance of various angle-ply fibre-reinforced composite beams subjected to a three-point bending test. Comprehensive analysis of the three-point bending test was performed to take into account various material responses in multi-layered composite beams that are characterized by different length-to-thickness ratios. The purpose of the conducted analysis is also to assess the impact of the type of fiber and its orientation on the flexural strength of various beam geometries. The numerical simulation of various three-point bending scenarios presented in this paper are found to be important before experimental study.

SUBJECT OF RESEARCH

Three-point bending test

The subject of this study is numerical strength analysis of angle-ply multi-layered fibre-reinforced composite beams subjected to the three-point bending test. Comprehensive analysis of the three-point bending test was performed to take into account various material responses and stress distributions in different beam types. What is important is the ratio between the support span and beam thickness (l/h) that affects the values of normal (tensile and compressive) and shear stresses along the beam length. Therefore, the length of the beam was selected in this study bearing in mind that the induced shear stresses decrease relative to the increase of the bending moment and l/h ratio. Furthermore, the aim of the bending tests is usually to determine the bending characteristics of a beam structure, and therefore high values of the support span-to-thickness ratio (l/h) are applied. According to the ASTM standard test method, those commonly used for three-point bending tests are 16:1 or 32:1, but ratios 40:1 and 60:1 are also specified to eliminate the shear effect [18]. In this study, two variants of loading conditions (referenced later in the paper as Variant 'a' and Variant 'b') are considered for a composite beam with layer orientations perpendicular and parallel to the loading plane (Fig. 1). Such an approach was used for comparison reasons and allowed the composite beam performance to be analysed when subjected to the three-point bending test in the two described loading variants.

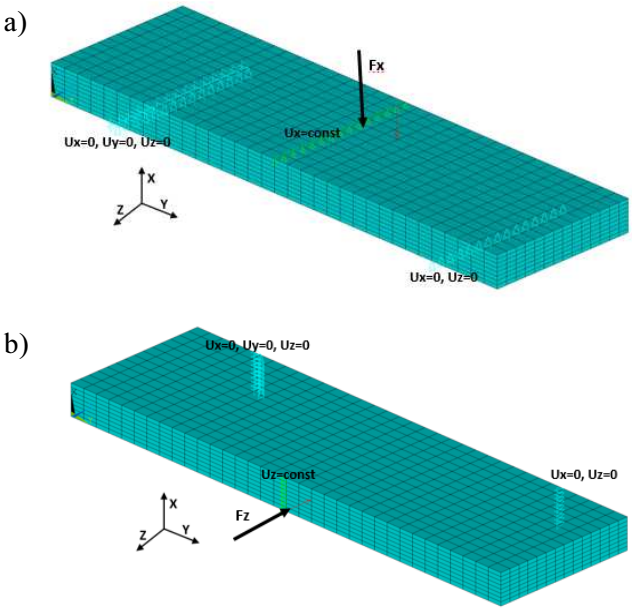

Fig. 1. Beam design with corresponding boundary conditions for loading conditions in Variant 'a' and Variant 'b'

Rys. 1. Projekt belki z warunkami brzegowymi dla obciążenia w Wariancie 'a' oraz Wariancie 'b'

Nevertheless, for the purpose of this study, three different beam types (I, II, III) were considered, for which the various span-to-thickness ratios (l/h) equal 4, 12, 32 for Variant 'a' and 0.8, 2.4, 6.4 for Variant 'b' respectively (Table 1). Herein, the height (h) and width (b) of the composite beam were assumed to be constant. The distance between the supporting pins and the beam ends (a) was assumed to be approx. 20% of the support span length.

TABLE 1. **Various beam types depending on *l*//*h* ratio**
TABELA 1. **Typy belek w zależności od stosunku *l*//*h***

	Beam type	Support span length *l* [mm]	Height *h* [mm]	Width *b* [mm]	Distance *a* [mm]
Variant 'a'	I l/h = 4	16	4	20	3.5
	II l/h = 12	48	4	20	10
	III l/h = 32	128	4	20	26
Variant 'b'	I l/h = 0.8	16	20	4	3.5
	II l/h = 2.4	48	20	4	10
	III l/h = 6.4	128	20	4	26

This study concerned the short beam shear (SBS) method that assumes the beam is short relative to its thickness. The aim was to increase the shear stresses in the laminate since it is claimed that for beam of ratios l/h = 4-5, the shear effect dominates the material response and provides high stress concentrations that initiate damage. In contrast, the span-to-thickness ratio

l/h = 32 provides the highest normal stresses, whereas for ratio l/h = 10-12 both the shear and normal stresses contribute significantly to beam failure [18]. Therefore, in the following study, three different beam geometries were taken into consideration to fully analyse the different variants of the three-point bending test. Such a comparative analysis allowed the author to investigate the flexural performance of the proposed composite beams with various shear and bending characteristics.

Loading conditions

There is a significant difference in the ratio of maximum normal stress (σ_{max}) to maximum shear stress (τ_{max}) for various beam geometries. According to classical beam theories, the maximum normal stress at the outer surface of the beam is given as:

$$\sigma_{\max} = \frac{6M}{bh^2} \tag{1}$$

where the maximum bending moment is defined as $M = \frac{Fl}{4}$.
The maximum shear stress at the mid plane is given as:

$$\tau_{max} = \frac{3V}{2bh} \tag{2}$$

for the shear force $V = \frac{F}{2}$ [19].

Consequently, the ratio of maximum normal stress to maximum shear stress for various beam types in Variants 'a' and 'b' can be expressed as the function of l/h as $\frac{\sigma_{max}}{\tau_{max}} = 2\frac{l}{h}$. This equals 8, 24, 64 for Variant 'a' and 1.6, 4.8, 12.8 for Variant 'b' in beam types I, II, III, respectively.

Composite material

A comparative study was performed simultaneously for two types of fibre-reinforced laminates, i.e., glass fibre reinforced polymers (GFRP E-glass/epoxy type) and carbon fibre reinforced polymers (CFRP carbon/epoxy type) [20]. Particularly, E-glass-epoxy and carbon-epoxy composites were taken into consideration. The analysis concerned an 8-layered composite beam for which the thickness of a single laminate was assumed equal to 0.5 mm. Additionally, depending on fibre orientations in the composite, four different layup configurations were distinguished: $[0_8]_T$, $[90_8]_T$, $[(45/-45)_4]_T$, $[(0/90)_4]_T$. Based on the literature review, appropriate elastic properties and strength limits were adopted for beams made of FRP material with transversally isotropic properties [20]. The properties of the multi-layered composite material were determined according to specific guidelines [21] in the main orthotropic directions that coincide with the fibre orientation (principal 1-axis) - see Table 2.

TABLE 2. **Mechanical properties of GFRP and CFRP composite [15, 20]**
TABELA 2. **Właściwości mechaniczne kompozytów typu GFRP oraz CFRP [15, 20]**

Mechanical properties	GFRP	CFRP
Longitudinal tensile modulus E_1 [GPa]	39	140
Transverse tensile modulus E_2 [GPa]	8.6	11
Shear modulus G_{12} [GPa]	3.8	5.5
Poisson's ratio ν_{12}	0.28	0.27
Longitudinal tensile strength X_t [MPa]	1080	2000
Longitudinal compressive strength X_c [MPa]	620	1200
Transverse tensile strength Y_t/ Z_t [MPa]	39	50
Transverse compressive strength Y_c/ Z_c [MPa]	128	170
Shear strength S [MPa]	89	70

NUMERICAL ANALYSIS

Numerical analysis was carried out using the FEM software package ANSYS®. The first stage of finite element analysis (FEA) required choosing the element type which allowed effective simulation of the material response of the composite beam subjected to the three-point bending test. In the analysis of thick-walled or curved multi-layered structures, the inter-laminar normal stresses (INS) might affect the flexural performance and beam failure modes. INS computation is not generally available in shell element formulations, which leads to the use of solid modelling instead [22]. Consequently, the SOLID185 element type was used to generate the 8-layered composite beam for which each layer was defined as a separate volume. Additionally, three elements were discretised along the layer thickness to take into account the inter-laminar bending effect. In each laminate a local coordinate system was created, which aligned the basis for material orthotropic directions in each element. As a result, the desired configurations of the composite layers were obtained: $[0_8]_T$, $[90_8]_T$, $[(45/-45)_4]_T$, $[(0/90)_4]_T$. Note that the material properties were defined in the model for GFRP and CFRP according to the mechanical characteristics given in [15]. For both materials the linear orthotropic model was applied wherein the X, Y, and Z labels of the material properties referred to the element coordinate system. Various beam geometries were modelled based on different support span-to-thickness ratios l/h (Table 1).

This study aimed to verify the performance of various beam geometries when subjected to the three-point bending test under different loading conditions. Hence, two variants of beam design with similarly defined boundary conditions (BC) were distinguished, i.e., load applied either perpendicular (Fig. 1a) or parallel (Fig. 1b) to the layer plane. Both variants were defined in the form of simply supported constraints which blocked appropriate kinematic degrees of freedom of beam specific points/lines. Herein, the nodes along the pinned

fastened support were fully constrained in translation, whereas the nodes for next one - the roller support were permitted to move in one direction along the surface upon which the roller rests. Displacement constraints were located appropriately along the beam length to assess various beam geometries. Arbitrarily, beam type II (l/h = 12 in Variant 'a' and l/h = 2.4 in Variant 'b') was chosen to reveal two variants of the assumed boundary conditions in Figure 1.

In each beam geometry bending was realized by applying a uniformly distributed load (of resultant F_x or F_z) along the line at the beam middle span. Herein, two types of loading were considered with force applied perpendicularly or parallel to the layer alignment in Variants 'a' and 'b' respectively. Specific nodes along the loaded line at the beam mid-span were also coupled (ux = const or uz = const) to guarantee that they would take the same displacement in the axial direction. Such a BC solution allowed the effect of stress concentration to be minimized at the regions where the load was introduced.

RESULTS AND DISCUSSION

Initially, numerical simulation of the three-point bending test estimated the deformed mode shapes of the various beam geometries subjected to flexural loading. Structural displacements were computed for three different beam types (I, II, III) in the direction coincident and perpendicular to the loading plane. The results are presented for GFRP material with fibre alignment $[0_8]_T$ in Figure 2 for Variant 'b' loading conditions. Such a comparative analysis showed considerably different deformed mode shapes for various beam geometries. The beam models for higher support span-to-thickness ratios (l/h = 6.4, l/h = 2.4) provided significantly higher middle-span deflection than the short beam (l/h = 0.8). The examined two variants of the three-point bending scenario predicted a considerable effect of the loading conditions on the beam flexural performance.

Geometrically nonlinear analysis was performed to estimate the equilibrium paths for the three-point flexural test. Solution in the full load range allowed the author to estimate the relationship between the load applied to the beam structure as the function of middle span deflection. As an example, a comparative analysis of two beam types (l/h = 4, l/h = 32) made of CFRP material is presented in Figure 3. For comparison reasons, the scales of the experimental bending curves predicted by FEA were limited to show only the relevant range. The results concern a beam subjected to the three-point bending test with load applied perpendicular to the layer plane (Variant 'a' boundary condition). Depending on fibre orientation, different laminate configurations were analysed: $[0_8]_T$, $[90_8]_T$, $[(45/-45)_4]_T$, $[(0/90)_4]_T$.

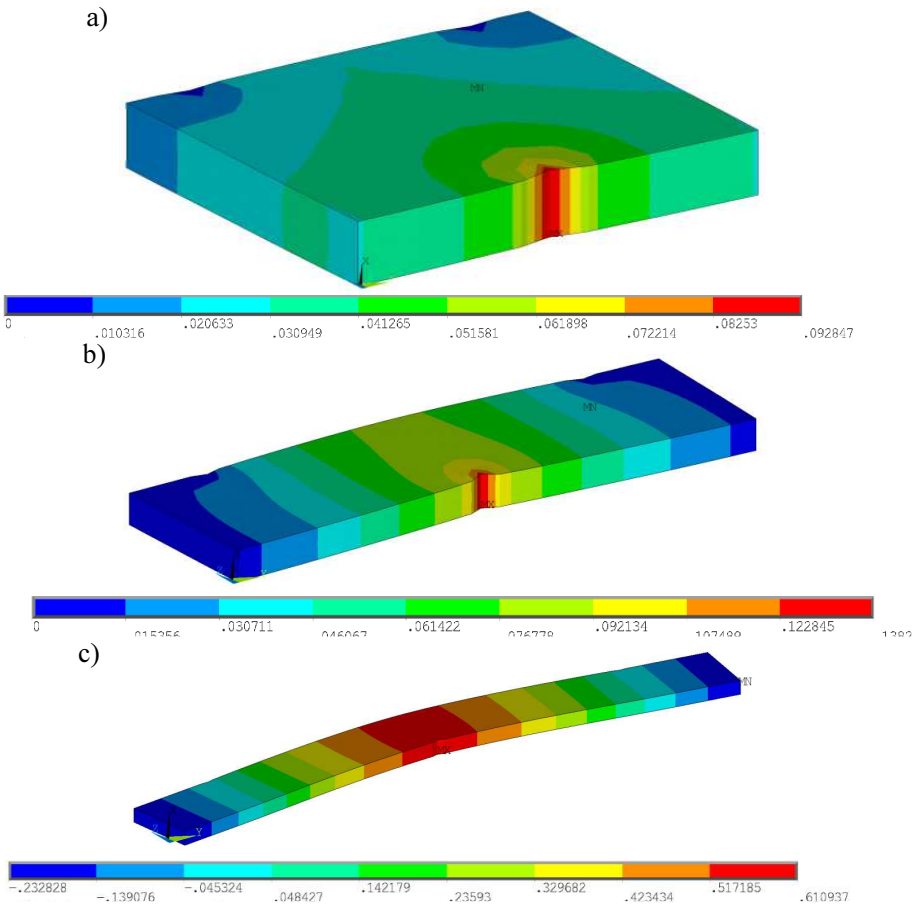

Fig. 2. Deformed modes for GFRP $[0_8]_T$ beam types: a) I (l/h = 0.8), b) II (l/h = 2.4), c) III (l/h = 6.4) in BC Variant 'b'

Rys. 2. Forma ugięcia dla belki GFRP $[0_8]_T$ typu: a) I (l/h = 0,8), b) II (l/h = 2,4), c) III (l/h = 6,4) z warunkami brzegowymi w Wariancie 'b'

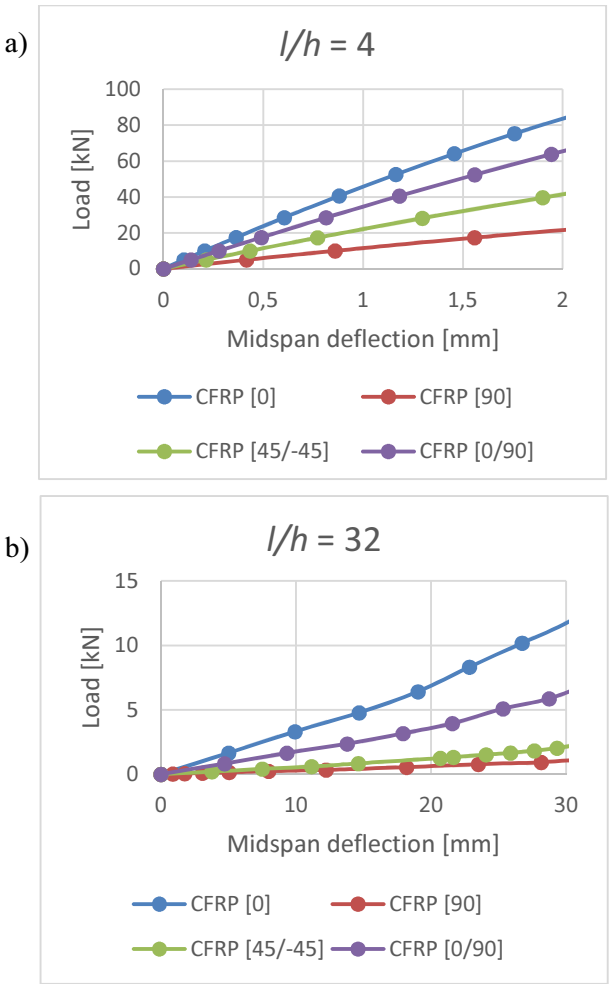

Fig. 3. Equilibrium paths for CFRP beam types: a) I (l/h = 4), b) III (l/h = 32) in BC Variant 'a'

Rys. 3. Ścieżki równowagi dla belki CFRP typu: a) I (l/h = 4), b) III (l/h = 32) z warunkami brzegowymi w Wariancie 'a'

For each considered beam type in various composite configurations, consistent results were achieved within the predicted equilibrium paths. Laminate $[0_8]_T$ was found to be the stiffest for each beam type ratio, whereas stacking sequence $[90_8]_T$ was the most susceptible to mid-span deflection when subjected to load perpendicular to the layer plane. The composite with fibre alignment $[(0/90)_4]_T$ was also found to be stiffer than the $[(45/-45)_4]_T$ layup. Such a comparative analysis for various sequences of laminate plies confirms the most considerable advantage of fibre-reinforced composites that can be designed to have the highest strength in a specific direction depending on the industrial application. Therefore, the presented comparative FE analysis of beam deflection for various beam geometries can provide composite manufacturers important insights. Depending on the mechanical properties of the different fibre types, comparative analysis was also conducted for GFRP and CFRP materials. For each beam type geometry, the GFRP material was found to be significantly more susceptible to deflection than the corresponding CFRP beams when subjected to the same loading conditions.

The load-midspan deflection curves were also predicted for Variant 'b' of boundary conditions with a layer orientation parallel to the loading plane. Two layup configurations ($[0_8]_T$ and $[90_8]_T$) were taken into consideration and compared for the GFRP material (see Fig. 4). The results confirmed that beams with higher support span-to-thickness ratios (l/h = 2.4, l/h = 6.4) provided significantly higher middle-span deflection than the short beam (l/h = 0.8). One can also notice various flexural responses for different composite layups in each beam type. For the short beam test (l/h = 0.8) the composite with the $[90_8]_T$ layup was found to be stiffer than the composite with the $[0_8]_T$ laminate stacking sequence. However, for longer beams (l/h = 2.4, l/h = 6.4) composite $[90_8]_T$ was more susceptible to deflection at the middle span. This results from the different stress distribution for various length beams, wherein the highest shear stresses for the assumed BC govern the material response in the short beam test.

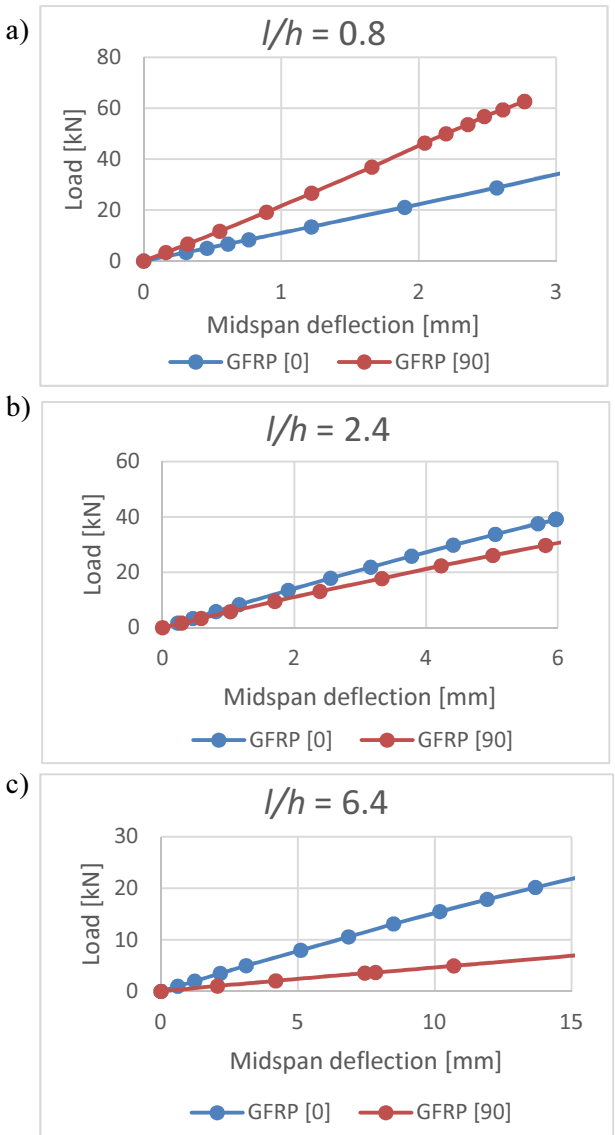

Fig. 4. Equilibrium paths for GFRP beam types: a) I (l/h = 0.8), b) II (l/h = 2.4), c) III (l/h = 6.4) in BC Variant 'b'

Rys. 4. Ścieżki równowagi dla belki GFRP typu: a) I (l/h = 0,8), b) II (l/h = = 2,4), c) III (l/h = 6,4) z warunkami brzegowymi w Wariancie 'b'

Based on the obtained results, it was noted that for load applied perpendicular to the layer orientation, layup $[0_8]_T$ was found to be the stiffest for each beam type ratio. However stacking sequence $[90_8]_T$ was the most deflected at the beam middle span for the corresponding load on each beam type. For load applied parallel to the layer orientation (Variant 'b'), the flexural response was not consistent for different composite layups in various beam types. Herein, for the short beam test ($l/h = 0.8$) the composite with the $[90_8]_T$ layup was found to be stiffer than the composite with the $[0_8]_T$ laminate stacking sequence. This is due to the loading direction in Variant 'b' that is coincident with the fibre orientation in 0 plies. However, as stated above different responses were obtained for the $l/h = 2.4$ and $l/h = 6.4$ beam types.

In order to validate the above numerical results achieved for the SOLID185 element type, the equilibrium paths were also estimated for another numerical model meshed with the SHELL181 element. As a result, the numerical computations performed for the beam ($l/h = 32$ or $l/h = 6.4$) predict the equilibrium paths in the same manner for both finite elements. Nevertheless, similar analysis performed in the full load range for the short beam ($l/h = 4$ or $l/h = 0.8$) indicates that geometry meshed with the shell element type is less susceptible to deflection than the solid type. It is due to the inter-laminar normal stresses (INS) which are not available in shell element formulations. As stated before, inter-laminar normal stresses induced for higher loads mainly affect beam performance in the case of thick-walled multi-layered structures such as one in the short beam test ($l/h = 4$ or $l/h = 0.8$). This also confirms that the more computationally expensive solid element type should be applied in beam flexural analysis. Nevertheless, an attempt should also be taken to perform the corresponding experimental tests to unambiguously analyse the obtained results and to validate the element types implemented in FEA.

CONCLUSIONS

This paper is a preliminary attempt to investigate GFRP and CFRP composite beams subjected to the three-point bending test by means of numerical simulations. The beam design was discussed for three different geometries depending on the beam support span-to-thickness ratio (l/h). Simulation of the three-point flexural test also included the short beam shear test (SBS), providing the beam is short relative to its thickness, which according to beam theory maximized the induced shear stresses. Various ply-stacking sequences were analysed in the simulations, which verified the beam performance based on the fibre alignment in the single composite layer. Geometrically nonlinear analysis allowed the author to estimate the load-midspan deflection curves for various beam types and laminate configuration. The predicted flexural performance was found to be a strong function of the ply-stacking sequence. The numerical simulation also analysed two finite element types i.e. SOLID185 and SHELL181 in order to validate the FE model and applied boundary conditions. It was verified that inter-laminar normal stresses (available in the SOLID185 computations) mainly affect beam flexural performance in the short beam test ($l/h = 4$ or $l/h = 0.8$). A negligible effect of the element type was observed for longer beams ($l/h = 32$ or $l/h = 6.4$), where the geometry discretized with the SHELL181 and SOLID185 types behaved alike when subjected to the considered three-point bending. This suggests that the more computationally-expensive solid element type should be considered especially in the case of short and thick-walled beams. However, at this stage numerical simulation of the GFRP and CFRP three-point testing method needs to be assessed by experimental evidence in order to validate the obtained results and to give other recommendations for its potential application.

Acknowledgments

This study was supported by the Ministry of Science and Higher Education of Poland - Diamond Grant No 0037/DIA/2017/46.

I would like to thank my supervisors Professors Zbigniew Kolakowski and Radosław Mania who provided insight and expertise that greatly assisted my research.

REFERENCES

[1] González C., Vilatela J.J., Molina-Aldareguía J.M., Lopes C.S., Lorca J., Structural composites for multifunctional applications: Current challenges and future trends, Progress in Materials Science 2017, 89, 194-251. DOI: 10.1016/j.pmatsci.2017.04.005.

[2] Rozylo P., Debski H., Wysmulski P., Falkowicz K., Numerical and experimental failure analysis of thin-walled composite columns with a top-hat cross section under axial compression, Composite Structures 2018, 204, 207-216. DOI: 10.1016/j.compstruct.2018.07.068.

[3] Banat D., Mania R.J., Stability and strength analysis of thin-walled GLARE composite profiles subjected to axial loading, Composite Structures 2019, 212, 338-345. DOI: 10.1016/j.compstruct.2019.01.052.

[4] Vlot A., Gunnink J.W., Fibre Metal Laminates: An Introduction, Springer Science & Business Media Dordrecht 2001.

[5] Czapski P., Kubiak T., Influence of fibre arrangement on the buckling load of composite plates - analytical solution, Fibres and Textiles in Eastern Europe 2015, 5, 92-97. DOI: 10.5604/12303666.1161764.

[6] Banat D., Kolakowski Z., Mania R.J., Investigations of fml profile buckling and post-buckling behaviour under axial compression, Thin-Walled Structures 2016, 107, 335-344. DOI: 10.1016/j.tws.2016.06.018.

[7] Banat D., Mania R.J., Failure assessment of thin-walled FML profiles during buckling and postbuckling response, Composites Part B: Engineering 2017, 112, 278-289. DOI: 10.1016/j.compositesb.2017.01.001.

[8] Czapski P., Kubiak T., Selected problems of determining critical loads in sructures with stable post–critical behaviour, Mechanics and Mechanical Engineering 2016, 20, 33-41.

[9] Valarinho L., Correia J.R., Branco F.A., Experimental study on the flexural behaviour of multi-span transparent glass-GFRP composite beams. Construction and Building Materials 2013, 49, 1041-1053. DOI: 10.1016/j.conbuildmat. 2012.11.024.

[10] Jakubczak P., Gliszczyński A., Bieniaś J., Majerski K., Kubiak T., Collapse of channel section composite profile subjected to bending Part II: Failure analysis, Composite Structures 2017, 179, 1-20. DOI: 10.1016/j.compstruct. 2017.07.052.

[11] Pahr D.H., Rammerstorfer F.G., Rosenkranz P., Humer K., Weber H.W., A study of short-beam-shear and double-lap-shear specimens of glass fabric/epoxy composites, Composites Part B: Engineering 2002, 33, 125-132. DOI: 10.1016/S1359-8368(01)00063-4.

[12] Schneider K., Lauke B., Beckert W., Compression shear test (CST) - a convenient apparatus for the estimation of apparent shear strength of composite materials, Applied Composite Materials 2001, 8, 43-62. DOI: 10.1023/A: 1008919114960.

[13] Shekar K.C., Prasad B.A., Prasad N.E., Interlaminar shear strength of multi-walled carbon nanotube and carbon fiber reinforced, epoxy – matrix hybrid composite, Procedia Materials Science 2014, 6, 1336-1343. DOI:10.1016/J.MSPRO. 2014.07.112.

[14] Sauvage J.-B., Aufray M., Jeandrau J.-P., Chalandon P., Poquillon D., Nardin M., Using the 3-point bending method to study failure initiation in epoxide-aluminum joints, International Journal of Adhesion and Adhesives 2017, 75, 181-189. DOI: 10.1016/j.ijadhadh.2017.03.011.

[15] Banat D., Load-carrying capacity of the GFRP and CFRP composite beams subjected to three-point bending test – numerical investigations, Mechanics and Mechanical Engineering 2019, 23, 277-286. DOI: 10.2478/mme-2019--0037.

[16] Czechowski L., Gliszczyński A., Bieniaś J., Jakubczak P., Majerski K., Failure of GFRP channel section beams subjected to bending - Numerical and experimental investigations, Composites Part B: Engineering 2017, 111, 112-123. DOI: 10.1016/j.compositesb.2016.11.057.

[17] Adams D., Lewis E., Experimental study of three- and four-point shear test specimens, Journal of Composites 1995, 17, 341-349.

[18] ASTM D790-03. Standard Test Method for Flexural Properties of Unreinforced and Reinforced Plastics and Electrical Insulation Materials. ASTM International 2003, 1-11.

[19] Liu C., Du D., Li H., Hu Y., Xu Y., Tian J. et al., Inter-laminar failure behavior of GLARE laminates under short-beam three-point-bending load, Composites Part B: Engineering 2016, 97, 361-367. DOI: 10.1016/j.compositesb. 2016.05.003.

[20] Hebda M., Zastosowanie energetycznego kryterium wytężeniowego do analizy wytrzymałościowej kompozytów włóknistych. PhD thesis, Cracow University of Technology, Cracow 2006.

[21] Barbero E.J., Finite Element Analysis of Composite Materials. 2nd ed. CRC Press, Boca Raton 2007.

[22] Li D., Qing G., Liu Y., A layerwise/solid-element method for the composite stiffened laminated cylindrical shell structures. Composite Structures 2013, 98, 215-227. DOI: 10.1016/j.compstruct.2012.11.013.

